JOURNAL OF MATERIALS SCIENCE 30 (1995) 3968–3972

Microstructure and electrical properties of YBCO thin films

Y. H. LI, C. LEACH, YUPU LI, J. A. KILNER, D. LACEY, A. D. CAPLIN
Centre for High Temperature Superconductivity, Imperial College, London SW7 2BP, UK
R. E. SOMEKH
Interdisciplinary Research Centre in Superconductivity, University of Cambridge, Cambridge, CB2 3QZ, UK

Microstructures of *c*-axis oriented YBCO thin films made by high-pressure d.c. sputtering on $LaAlO_3$ and MgO substrates were examined by TEM. The *a*-axis oriented grains, second phases and micro-twins were frequently observed in the film. The *a*-axis oriented grains expanded along their *c*-axis directions during film growth. The *a*- and *b*-axis misorientations were observed in the film on MgO due to serious lattice mis-match between YBCO and MgO. The second phases were often accompanied with *a*-axis oriented grains suggesting they act as nuclei. These observed results were correlated with the measured T_c and J_c of the films.

1. Introduction

High-T_c superconductors hold great promise for applications in the field of high-frequency electronics. The crystalline quality achieved in thin films of the superconductor YBCO makes critical current densities in the order of 10^7 A cm^{-2} possible [1], and results in a microwave surface resistance at 90 GHz, a factor of 10 smaller than that of copper at 77 K [2]. Epitaxial YBCO thin films have been grown by many different techniques on a number of lattice-matched single-crystal substrates [3–6]. However, because the differences in lattice constants for *a*, *b* and *c*/3 of YBCO are very small, most of the YBCO thin films on [1 0 0] perovskite substrates have a mixture of epitaxial grains with *a*-axis, *b*-axis or *c*-axis normal to the surface [7–10]. This tendency to form mixed epitaxial grains seriously affects surface smoothness of the film caused by the difference in growth rates parallel to, and normal to, the *c*-axis [11], making them unsuitable for many applications [12–14] when they are grown within a narrow range of conditions for the best transport properties [15]. A detailed understanding of the growth mechanism and the ability to control the microstructure are key issues for successful device application. In this work we concentrate on the microstructure and its influence on the electrical properties.

2. Experimental procedure

YBCO films were made by using high-pressure d.c. sputtering. Pure oxygen gas was used for the film deposition. The deposition temperature was 780–800 °C. The other conditions were as given in Table I.

Plan view TEM samples were made by mechanical thinning, dimpling and ion-milling from the substrate side. Cross-section samples were prepared by gluing the samples face to face together. After mechanical thinning the samples were dimpled to about 10 μm thickness in the central region and ion-milled to perforation. The TEM samples were observed on a JEOL 2010.

The T_c for the films was measured by a.c. susceptibility [16]. The resistive curve was obtained by a standard four-terminal Van der Pauw measurement. The magnetization critical current density, J_c, was measured by using a vibrating sample magnetometer (VSM). The samples were also characterized by X-ray diffraction (copper target, K_α irradiation) on a Philips PW 1730 instrument.

3. Results and discussion

3.1. YBCO film on $LaAlO_3$ (1 0 0)

The thickness of the film measured across a step edge by a Talystep stylus profilometer varied from 180–340 nm. Fig. 1a shows a typical plan-view image of sample 1, the YBCO film on $LaAlO_3$. The electron diffraction pattern observed for this sample suggests that it is mainly *c*-axis oriented epitaxial single crystal which is shown in Fig. 1b. The selected area covered the whole image (i.e. a few micrometers of the observed area). The diffraction pattern also shows that

TABLE I YBCO film deposition condition

Sample	Substrate	Sputter pressure (Pa)	Target–substrate distance (mm)	Sputter time (h)
1	$LaAlO_3$	300	11	2
2	MgO	300	11	2.5
3	MgO	225	15	1

0022–2461

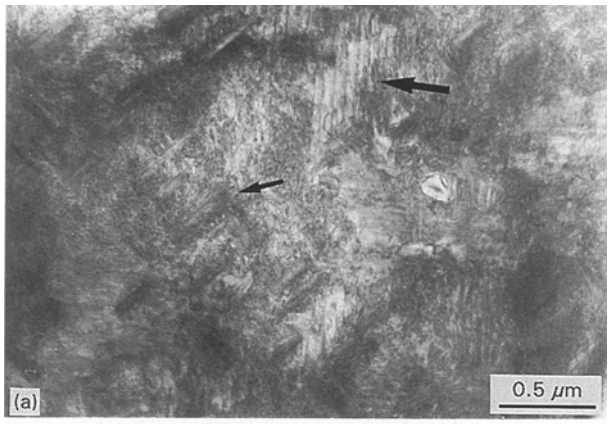

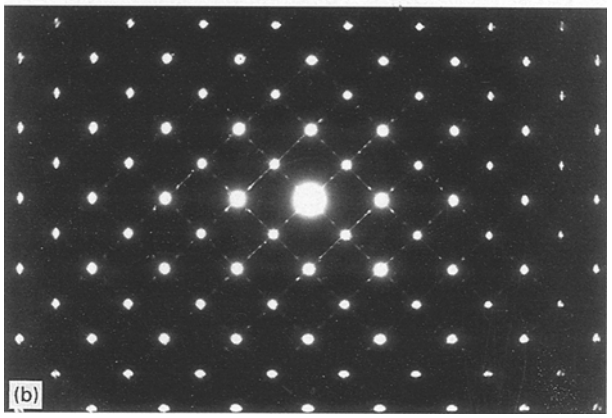

Figure 1 A typical plan-view image and its electron diffraction pattern of sample 1.

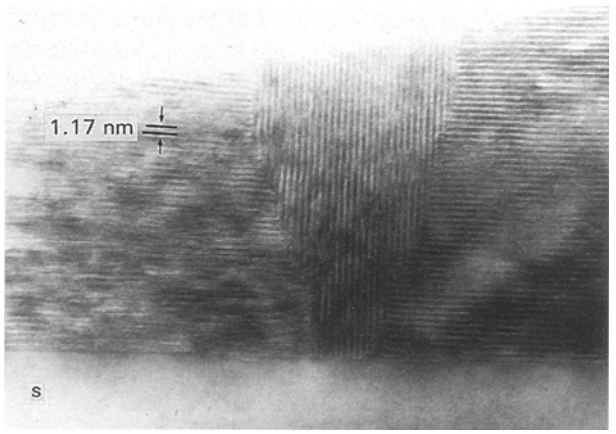

Figure 2 A high-resolution cross-sectional image of an *a*-axis oriented grain in sample 1.

between the much stronger spots for the *c*-axis orientation there are some weak spots evident, which correspond to *a*-axis oriented grains. In the image some needle-shaped *a*-axis oriented grains (as indicated by a small arrow) and some micro-twins with regular intervals of about 50 nm (as indicated by a large arrow) can be seen. The existence of the micro-twins can also be confirmed from the diffraction pattern, which shows a splitting of the main diffraction spots. A high-resolution cross-sectional image of an *a*-axis oriented grain is shown in Fig. 2. It can be seen that the interface between YBCO and $LaAlO_3$ is quite

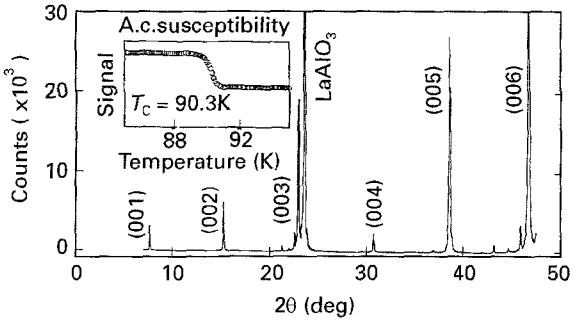

Figure 3 The X-ray diffraction pattern and the inductive transition of sample 1.

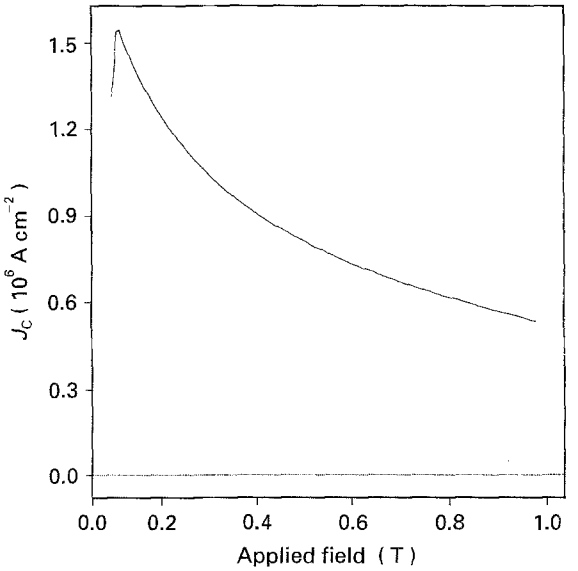

Figure 4 The J_c of sample 1 as a function of applied field, $B(T)$, at 70 K.

smooth. The upper part of the grain is wider than that of the lower part, which is the result of growth competition between the grain and the surrounding *c*-axis oriented film. It should be noted that within a distance of 10 nm from the substrate (indicated by S), there is no expansion of the grain along its *c*-axis direction. This implies that the initial growth of the *a*-axis oriented grain was confined along the *a*- and *b*-axes only. As has been shown in Fig. 1, the *a*-axis oriented grains are needle shaped, which suggests that the growth rates along the *a*- and *b*-axes are much higher than that along the *c*-axis. Therefore, during the growth of the film it is expected that at some stage the *a*-axis oriented grain would grow above the surrounding *c*-axis oriented single-crystal surface. Only at this stage, will the *a*-axis oriented grain begin its expansion along its *c*-axis direction. This *a*-axis grain out-growth above the film surface had been observed by another group [17].

The X-ray diffraction pattern observed using CuK_α radiation and an automated independent theta and two theta diffractometer confirms that the film is mainly *c*-axis oriented (Fig. 3). The *c*-axis length and the oxygen content $(7 - x)$ calculated from this length [18] are equal to 1.167 nm and 6.97, respectively. The insert in Fig. 3 shows the inductive transition of the

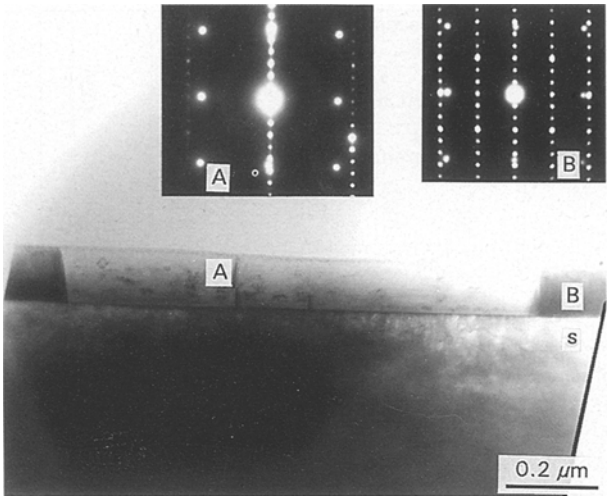

Figure 5. A cross-sectional image of an *ab*-axis misoriented grain and its electron diffraction pattern in sample 2.

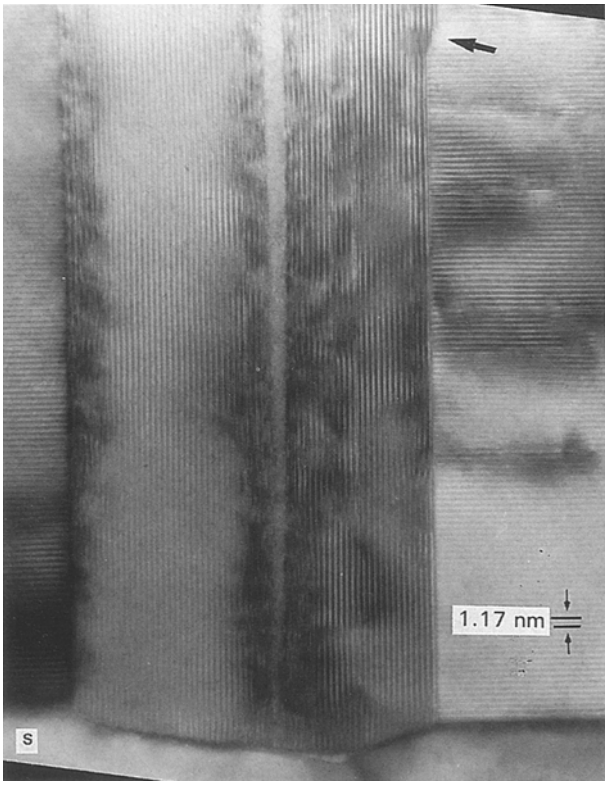

Figure 6 A high-resolution cross-sectional image of an *a*-axis oriented grain in sample 2.

sample, measured from the real part of the magnetic susceptibility, (χ'). T_c (i.e. zero resistance) was found to be 90.3 K as determined from the peak of dV/dT [15]. The value of T_c (i.e. 90.3 K) is near the highest T_c obtained for sputtered YBCO films on $LaAlO_3$. To our knowledge, it is difficult to make a sputtered YBCO film with the optimum T_c (i.e. 92 K) of the 123 phase. Fig. 4 shows J_c of the sample as a function of applied field $B(T)$ at 70 K.

3.2. YBCO film on MgO (100)

The microstructure of the YBCO film MgO (sample 2) observed on plan-view and cross-sectional samples is

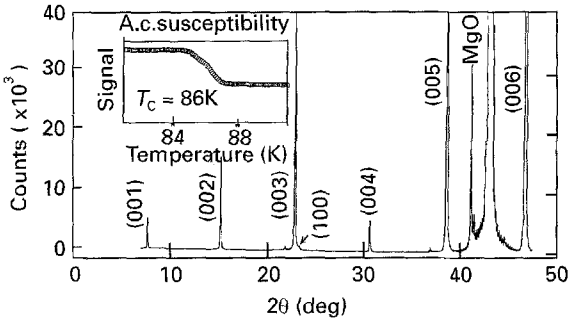

Figure 7 The X-ray diffraction pattern and the inductive transition of sample 2.

similar to that described for sample 1 except that some *c*-axis oriented grains were observed with rotation along its *c*-axis relative to the surrounding *c*-axis epitaxial film. A cross-sectional image of this grain is shown in Fig. 5. This could be due to the 9% lattice mismatch between YBCO and MgO which is larger than the lattice mismatch between YBCO and $LaAlO_3$ of $< 3\%$. This mismatch is shown in the inserted diffraction patterns, in which the isolated bright spots are from MgO substrate. The film thickness is about 150 nm determined from the picture. The diffraction pattern (A) in Fig. 5 was taken from the bright area on the film including some part of the substrate (indicated by S), which shows that the *c*-axis of this grain is still normal to the substrate, but the *a*-axis is not parallel to the *a*-axis of the substrate, which is the *a*-axis direction of the most part of the film as shown in the diffraction pattern (B). The [2 1 0] direction of this grain is normal to the photo. A high-resolution cross-sectional image of an *a*-axis oriented grain in the film shown in Fig. 6. The surface smoothness of the interface between MgO and YBCO is not as good as that observed for sample 1. The grain seems to have grown from a small concave feature on the substrate. It would thus take a longer time for this grain to grow over the surrounding surface during film growth, which resulted in a long distance (about 100 nm) from the substrate where the grain began the expansion along its *c*-axis direction (indicated by an arrow). It can be seen also that within the grain there is a narrow strip which is not resolved. This could be a second phase or the same phase with different orientation. There is also a dislocation leading into the bottom of the MgO surface pit.

The X-ray diffraction pattern of the sample (Fig. 7) shows that the film is still mainly *c*-axis oriented with some *a*-axis oriented grains (a small (1 0 0) peak is indicated by an arrow). This suggests that there are not many *c*-axis oriented grains with an *ab*-axis misorientation. T_c for this film was also measured by a.c. susceptibility and found to be 86 K, as shown in the insert to figure. Normally YBCO films on MgO made by this technique are found to have a lower T_c than those on $LaAlO_3$.

Fig. 8 shows a plan-view image of a different YBCO film on MgO (sample 3) which has a film thickness of about 80–150 nm. It can be seen in the image that even though majority of the film is *c*-axis oriented there are

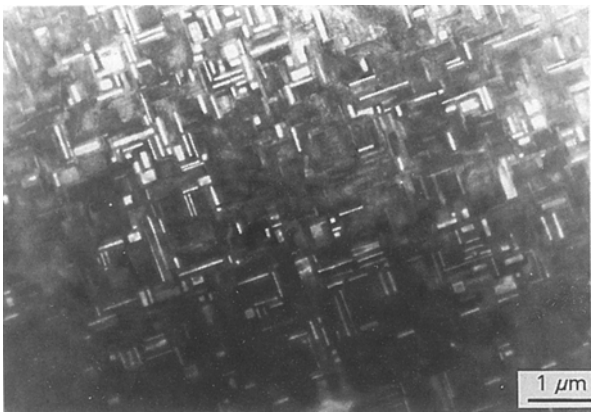

Figure 8 A plan-view image of sample 3.

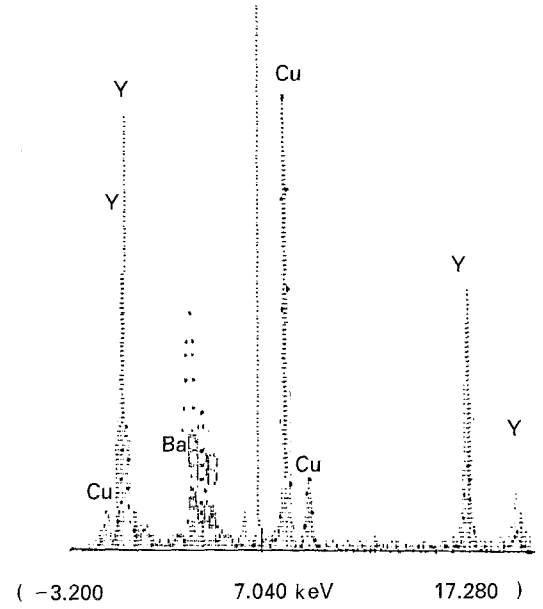

Figure 9 An EDS spectrum of second phases in sample 3.

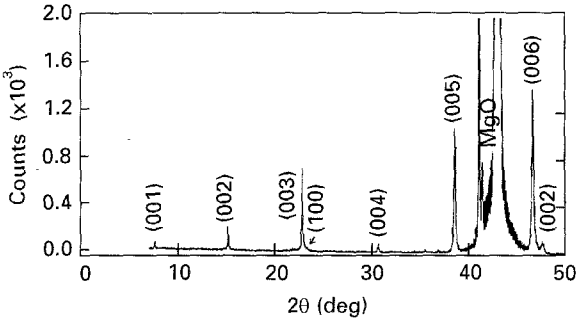

Figure 10 The X-ray diffraction pattern of sample 3.

some second-phase regions (bright regions) in the film and these are surrounded by needle-shaped *a*-axis oriented grains. EDS analysis indicates that this second phase is yttrium-rich and barium-poor compared with the 123 phase as shown in Fig. 9, in which the dotted curve is a spectrum collected from a nearby 123 phase. The micro-beam diffraction pattern suggests that these second phases have a polycrystalline structure. This implies that the *a*-axis oriented grains nucleate preferentially at regions in the film which are

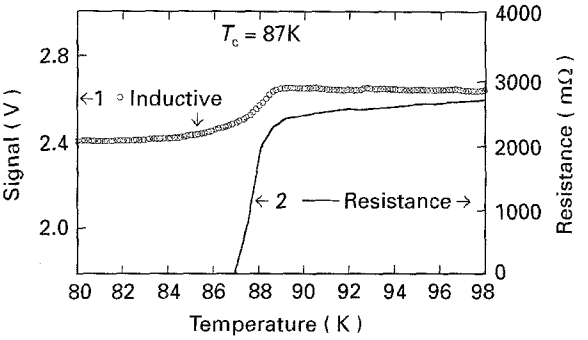

Figure 11 The T_c of sample 3 measured by inductive and resistance methods.

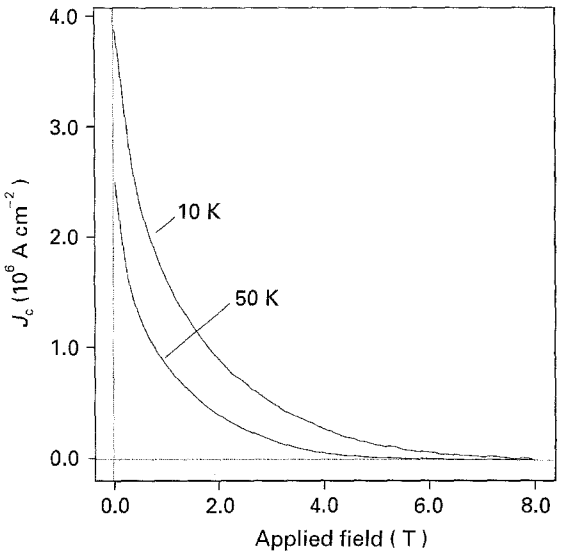

Figure 12 The magnetization J_c of sample 3.

off-stoichiometry and, once *a*-axis oriented grains were formed, they slow down the horizontal expansion of the 123 phase because the growth rate along the *c*-axis of the 123 phase is much slower than that along the *a*- and *b*-axes.

The X-ray diffraction pattern of the sample 3 shows a small (1 0 0) peak from the *a*-axis oriented grains as shown in Fig. 10 (indicated by an arrow). The T_c was again measured using a.c. susceptibility and resistance method and found to be 87 K as shown in Fig. 11. Fig. 12 shows the magnetization J_c, of this sample. It can be seen J_c is quite low, probably because the magnetization current is limited by the boundaries of the *a*-axis grains and second phases.

4. Conclusion

The *a*-axis oriented grains, second phases and microtwins were frequently observed in the *c*-axis oriented YBCO films on $LaAlO_3$ and MgO substrates. The *a*-axis oriented grains expanded along their *c*-axis directions during film growth. But there were no expansions during the initial film growth, and the position where they started to expand depended on the smoothness of the substrate. The *a*- and *b*-axis misorientations were observed in the film on MgO, but not on $LaAlO_3$. The second phases were often accom-

panied with *a*-axis oriented grains suggesting they act as nuclei. The T_c and J_c of the film on MgO are not as good as on $LaAlO_3$.

Acknowledgement

This work was supported by the UK Engineering and Physical Science Research Council.

References

1. J. GEERK, G. LINKER and O. MEYER, *Mater. Sci. Rep.* **4** (1989) 193.
2. N. KLEIN, G. MULLER, H. PIEL, B. ROAS, L. SCHULTZ, U. KLEIN and M. PEINIGER, *Appl. Phys. Lett.* **54** (1989) 757.
3. P. M. MANKIEWICH, J. H. SCOFIELD, W. J. SKOCPOL, R. E. HOWARD and A. H. DAYEM, *ibid.* **51** (1987) 1753.
4. S. WITANACHCHI, H. S. KWOK, X. W. WANG and D. T. SHAW, *ibid.* **53** (1988) 234.
5. C. B. EOM, J. Z. SUN, K. YAMAMOTO, A. F. MARSHALL, K. E. LUTHER, T. H. GEBALLE and S. S. LADERMAN, *ibid.* **55** (1989) 595.
6. Y. H. LI, C. LEACH and P. G. QUINCEY, *J. Mater. Sci. Lett.* **14** (1995) 670.
7. C. H. CHEN, J. KWO and M. HONG, *Appl. Phys. Lett.* **52** (1988) 841.
8. J. D. BUDAI, R. FEENSTRA and L.A. BOATNER, *Phys. Rev.* **B39** (1989) 12355.
9. S. W. CHAN, D. W. HWANG and L. NAZER, *J. Appl. Phys.* **65** (1989) 4719.
10. D. M. HWANG, T. VENKATESAN, C. C. CHANG, L. NAZAR, X. D. WU, A. INAM and M.S. HEGDE, *Appl. Phys. Lett.* **54** (1989) 1702.
11. B. M. CLEMENS, C. W. NIEH, J. A. KITTL, W. L. JOHNSON, J. Y. JOSEFOWICZ and A. T. HUNTER, *ibid.* **53** (1988) 1871.
12. C. C. CHANG, X. D. WU, A. INAM, D. M. HWANG, T. VENKATESAN, P. BARBOUX and J.M. TARASCON, *ibid.* **53** (1988) 517.
13. T. VENKATESAN, C. C. CHANG, D. DIJKKAMP, S. B. OGALE, E. W. CHASE, L. A. FARROW, D. M. HWANG, P. F. MICELI, S. A. SCHWARTZ, J. M. TARASCON, X. D. WU and A. INAM, *J. Appl. Phys.* **63** (1988) 4591.
14. G. KOREN, R.J. BASEMAN, A. GUPTA, M.I. LUTWYCHE and R. B. LAIBOWITZ, *Appl. Phys. Lett.* **56** (1990) 2144.
15. D. H. A. BLANK, D. J. ADELERHOF, J. FLOKSTRA and H. ROGALLA, *Phys. C* **169** (1990) 423.
16. F. J. MULLER, J. C. GALLOP and A. D. CAPLIN, *Supercond. Sci. Technol.* **4** (1991) 616.
17. H. TAKAHASHI, Y. AOKI, T. USUI, R. FROMKNECHT, T. MORISHITA and S. TANAKA, *Phys. C* **175** (1991) 381.
18. A. KUPLA, A. C. P. CHAKLADER, G. ROENER and D. LI, *Supercond. Sci. Technol.* **3** (1990) 483.

Received 2 February
and accepted 22 March 1995